

# Gravitational wave

**Detection and observation of gravitational waves requires extremely accurate displacement measurement in the frequency range of 0.03 mHz to 1 Hz. The Laser Interferometer Space Antenna (LISA) mission will attain this by creating a giant interferometer in space, based on free-floating proof masses in three spacecrafts. Due to orbit evolution and time delay in the interferometer arms, the direction of transmitted light changes. To solve this problem, a picometer-stable Point-Ahead Angle Mechanism (PAAM) was designed, realized and successfully tested.**

• **Joep Pijenburg and Niek Rijnveld** •

**T**he picometer-stable scan mechanism is a crucial element in the Laser Interferometer Space Antenna (LISA) mission [1] [2]. The objective of the LISA mission is to observe and measure gravitational waves. Because of the extreme stability and low disturbance requirements, the detector will be created in space. The detector will consist of a giant interferometer with three measurement arms, travelling between three spacecrafts each at a distance of 5 million kilometers from each other; see Figure 1. Each spacecraft holds two free-floating proof masses, which provide the absolute reference for the interferometer arms. Because the disturbances acting on the proof masses have been absolutely minimized, any path length changes measured by the interferometer arms can be attributed to gravitational waves.

Due to the evolution of the orbit during its trip around the sun, the laser beam angles have to be corrected for constantly. Not only the in-plane angles are affected, but also the so-called point-ahead angles, which correct for the offset caused by the time delay of the travelling light. The Point-Ahead Angle Mechanism (PAAM) is designed to

perform the task of correcting the point-ahead angle. The PAAM was developed and tested by TNO Science & Industry, with the help of the Albert Einstein Institution in Hannover, Germany. As an Elegant Bread Board (EBB), it has successfully gone through all performance and environmental testing and is ready to be integrated in a functional breadboard of the Optical Bench for a LISA spacecraft.

## Authors

Joep Pijenburg and Niek Rijnveld are members of the Precision Motion Systems Department of TNO Science and Industry in the Netherlands. The LISA mission is a combined ESA NASA space mission. The Point Ahead Angle Mechanism was developed by TNO in a technology development programme under contract of the European Space Agency (ESA).

[www.tno.nl](http://www.tno.nl)

# detection in space

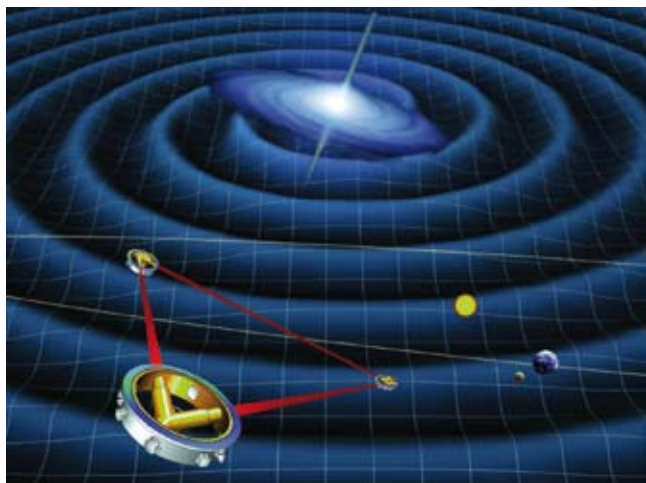


Figure 1. Artist impression of the LISA mission. (Illustration: NASA)

## Driving requirements

The PAAM is required to steer the incoming laser beam through a range of  $\pm 824 \mu\text{rad}$ , while contributing minimally to the optical path delay (OPD) as well as to the angular jitter of the laser beam angle. During operation, the mechanism will follow an annual trajectory that runs through the entire range twice.

## Performance requirements

Both the specification for the optical path delay (OPD) and the angular jitter were described using a noise shape function, as shown in Equation 1.

$$n(f) = \sqrt{\left(1 + \frac{2.8 \text{ mHz}}{f}\right)^4} \quad (1)$$

The requirements for OPD and angular jitter, defined in terms of amplitude spectral density (ASD), were multiplied with this noise shape function. It has been designed such that the requirements are relieved below 2.8 mHz, and constant above this frequency. The requirements only apply within the LISA measurement bandwidth, which is defined to be between 0.03 mHz and 1 Hz. Table 1 shows the requirements for OPD and angular jitter.

Table 1. Performance requirements for the PAAM.

Description	Requirement	Unit
Optical Path Delay	$1.4 \cdot n(f)$	$\text{pm}/\text{Hz}^{1/2}$
Angular jitter	$16 \cdot n(f)$	$\text{nrad}/\text{Hz}^{1/2}$

## Environmental requirements

Several additional requirements made the design of the PAAM quite challenging. First of all, due to the sensitivity of the measurement set-up on the Optical Bench, no magnetic materials were allowed. This ruled out the use of any electromagnetic actuators or bearings. Second, due to the strict requirements on stray light, the contamination requirements on the Optical Bench were extremely strict. Any outgassing materials, as well as mechanisms containing moveable parts with frictional contacts were to be avoided. Third, the mechanism will have to survive launch loads of 25 g RMS, without the use of a launch locking mechanism.

## Design description

The PAAM consists of a mirror on a flexible rotational hinge, which can be actuated individually by either one of two piezo stacks. The angle is measured by a capacitive sensor. The system operates in closed loop. The overall design is shown in Figure 2, and its realization is shown in Figure 3. In the paragraphs below, the optical, mechanical and electrical design is described in detail.

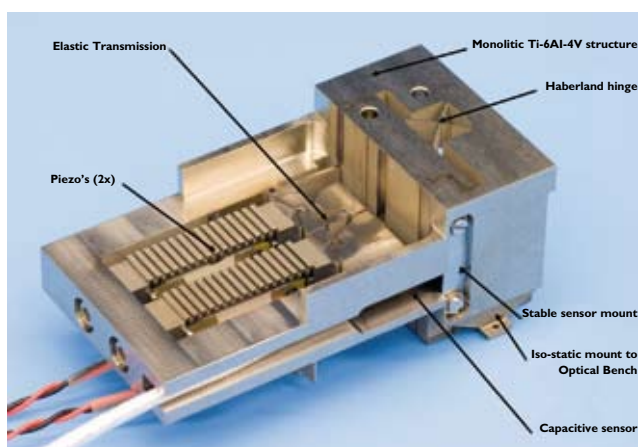


Figure 2. Elegant Bread Board of the Point-Ahead Angle Mechanism as designed by TNO Science and Industry, including all its components. (Photo courtesy of Leo Ploeg)

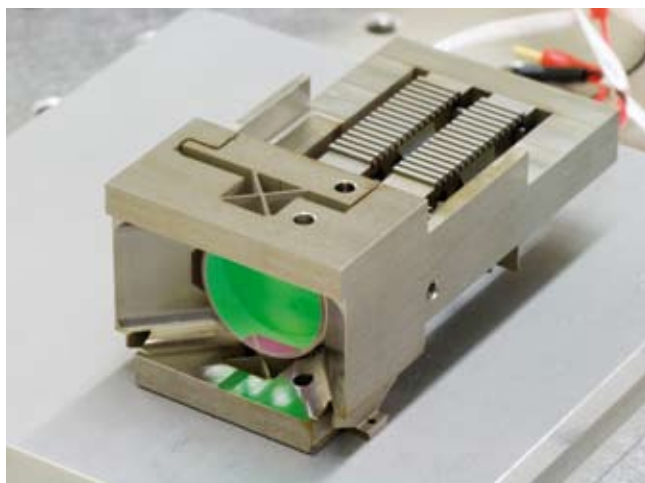


Figure 3. Realization of the PAAM. The mirror is glued to a monolithical structure featuring a Haberland hinge. The mirrors can be actuated by one of two piezo stacks. (Photo courtesy of Leo Ploeg)

**Optical design**

The optical concept for the PAAM is a mirror rotating around an axis in the mirror plane. This concept was chosen over alternatives due to its low transmission losses and low complexity. The mirror is coated for the wavelength of 1064 nm and for the incoming angle of 45°. The reflectivity is specified as more than 99.9%, and its flatness is better than 12 nm RMS over its entire diameter of 19.05 mm.

The Optical Path Delay (OPD) has been identified as the most critical requirement. If the laser beam and the reflecting surface are perfectly aligned with the rotation, the OPD due to rotation is theoretically zero. Figure 4 schematically shows the optical path delay due to a rotation of the mirror, when the beam and surface are not perfectly aligned.

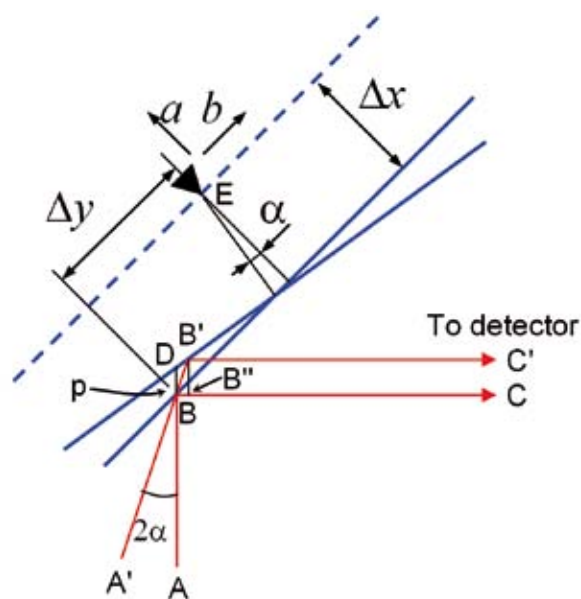


Figure 4. Schematic representation of the influence of alignment and jitter parameters of the mirror on the optical path delay of the incoming laser beam.

From Figure 4 it can be seen that the OPD equals the distance  $BB' - BB''$ . For small angles, this can be approximated by  $BD$ . The sensitivity of the distance  $BD$ , and hence the OPD, to the most relevant parameters is listed in Table 2. These parameters are the angular jitter, caused by rotation of the mirror around the optical axis in combination with an alignment offset, the longitudinal jitter, caused by piston sensitivity and angular jitter, and the rotation axis longitudinal jitter, caused by parasitical actuation forces through the Haberland hinge. Other misalignments of the optical axis and cross-couplings were shown to have negligible contribution to the optical path delay.

**Mechanical design**

The rotation of the mirror is guided by a so-called Haberland hinge, a monolithical elastic cross hinge. Due to the restrictions on magnetic materials and contamination, magnetic, hydrostatic or contact bearings are not favored. The axis of rotation of the Haberland hinge is aligned with the mirror surface. As the material  $Ti_6Al_4V$  was selected, due to its high allowable stress and high dimensional

Table 2. Sensitivity of the OPD to relevant parameters

Parameter	Description	Budget	Relation	Effect on OPD (pm/Hz <sup>1/2</sup> )
$\Delta x$	Static longitudinal misalignment	$\pm 1000 \mu m$	-	0
$\Delta y$	Static lateral misalignment	$\pm 50 \mu m$	-	0
$\Delta \alpha$	Angular jitter	$8 \cdot n(s) \text{ nrad/Hz}^{1/2}$	$\delta BD = 2^{1/2} (\Delta x \alpha + \Delta y) \delta \alpha$	$0.57 \cdot n(s)$
$\delta \Delta x$	Longitudinal jitter	$0.28 \cdot n(s) \text{ pm/Hz}^{1/2}$	$\delta BD = 2^{1/2} (1 + 0.5 \alpha^2) \delta \Delta x$	$0.40 \cdot n(s)$
$\delta \alpha$	Rotation axis longitudinal jitter	$0.30 \cdot n(s) \text{ pm/Hz}^{1/2}$	$\delta BD = 2^{1/2} \delta \alpha$	$0.43 \cdot n(s)$
Total				$1.40 \cdot n(s)$

stability. The mechanical design is shown in Figure 3. The entire mechanism, excluding the functional components, was wire-eroded in a single fixture configuration; such that optimal production tolerances were achieved.

A compact elastic transmission between the actuator and mirror allows actuation of the mirror angle without introducing parasitic forces. The elastic transmission also enabled the inclusion of a second, independent actuator, such that the mechanism is redundant. The required mechanical stroke of  $\pm 412 \mu\text{rad}$  can be actuated with an actuator stroke of  $20 \mu\text{m}$ , with minimal hysteresis effects. To minimize OPD due to temperature variations, the thermal centre of the  $\text{Ti}_6\text{Al}_4\text{V}$  structure was placed in line with the axis of mirror rotation. This was achieved by strategic placement of isostatic interfaces to the optical bench.

A finite-element model analysis (FEM) of the Haberland hinge was used to predict the longitudinal jitter, caused by the coupling between angular jitter and piston sensitivity. Production tolerances of  $\pm 10 \mu\text{m}$  were included, which was justified by the accuracy and symmetry of the applied wire-erosion process to manufacture the monolithical mechanism. Figure 5 shows the calculated piston movement of the mirror rotation axis under different actuation angles. The derivative of this curve is the piston sensitivity to angular jitter, which is  $2.1 \text{ fm/nrad}$  at the maximum angle. With the requirement of  $8 \text{ nrad/Hz}^{1/2}$ , the predicted longitudinal jitter becomes  $0.017 \text{ pm/Hz}^{1/2}$ , which is significantly below the allocated budget of  $0.28 \text{ pm/Hz}^{1/2}$ .

#### Electrical design

For the actuation, two piezo stacks (PPA20M) of Cedrat Technologies were selected. For the stroke of  $20 \mu\text{m}$ , and with the limitations on magnetic materials, a piezo stack is the most appropriate actuator. The stacks are driven with a high-voltage piezo amplifier (Cedrat Technologies LA75B), which produces voltages between  $-20$  and  $+150 \text{ V}$ .

Because of piezo hysteresis and discharge behaviour, a closed-loop system was required to meet the requirement for angular jitter in the entire range. The controller acting between the sensor and piezo actuator can have a low bandwidth, because only disturbances within the LISA measurement bandwidth have to be suppressed.

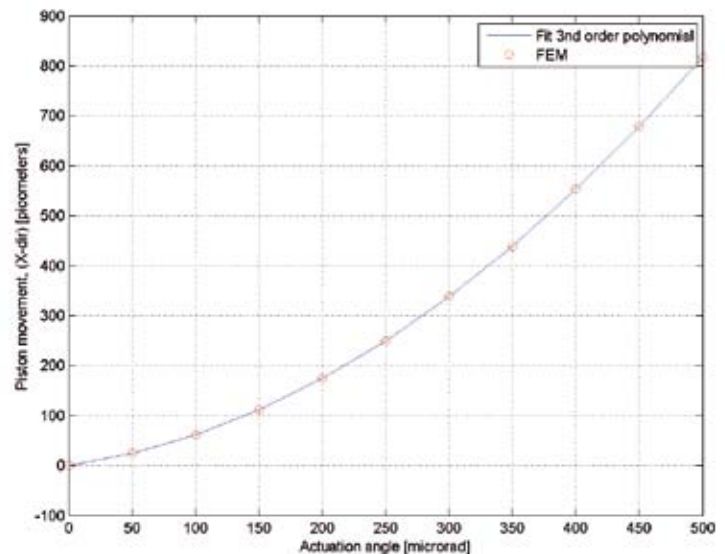


Figure 5. The piston movement of the axis of rotation under different actuation angles. By taking the derivative of the fitted polynomial, the piston sensitivity can be determined for different angles.

The sensor consists of an active target capacitive sensor system, which measures the displacement of the far end of the mirror (see Figure 6). The tilting of the mirror is less than  $0.5 \text{ mrad}$ , which has only a small influence on the capacitive sensor signal. A one-time calibration ensures that the sensor signal is representative of the mirror angle with high enough accuracy. The active target system is preferred over a passive target system for the following reason: in a passive target system, the cable capacitance is in parallel to the capacitance to be measured, and is typically a few orders higher. This makes it very sensitive to low-frequency environmental changes which dramatically influence the cable capacitance. In an active target system, the target is connected to a virtual ground, which draws the current from the cable capacitance. This way, the system will be much less sensitive to environmental changes.

The capacitive probe is a standard Lion Precision probe, whereas the active target consists of an isolating BK7 plate, coated with a layer of gold. The active target, located on the moving part, was connected to the sensor cable by two thin copper wires, which add negligible parasitic stiffness to the Haberland hinge. The capacitance-to-digital converter (CDC) electronics were chosen to be a custom electronics board, especially for extreme requirements on low-frequency noise. Typically, capacitive sensor electronics introduce  $1/f$  type noise in the amplification, but the charge-integration configuration and precision electrical components chosen for the CDC board reduce this effect maximally.

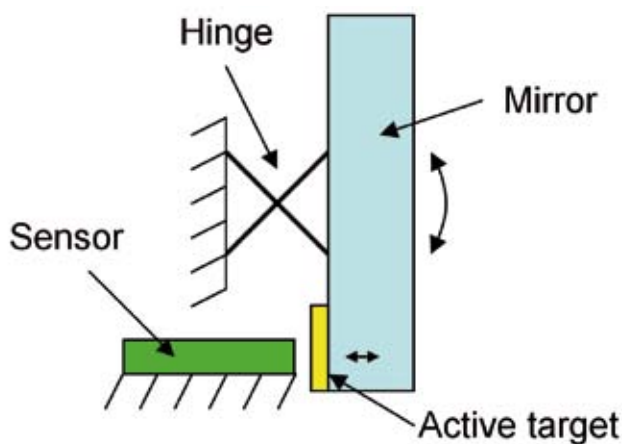


Figure 6. Schematic illustration of the active target capacitive sensor. The sensor measures the displacement of the tip of the mirror. The tilting of the mirror is taken into account by one-time calibration.

### Performance testing

Before and after the environmental test, consisting of 25 g RMS random vibrations and thermal cycling from 0 to 80 °C, the performance of the PAAM Elegant Bread Board was measured. This was done with the help of the Albert Einstein Institution in Hannover, because of their experience with measuring picometer stabilities and the availability of an existing measurement facility [3].

Figure 7 shows the test set-up used for the performance measurements, featuring a vacuum chamber pumped down to  $10^{-4}$  mbar that is temperature controlled to less than  $14 \mu\text{K}/\text{Hz}^{1/2} \cdot n(f)$ . The extreme stability required to measure  $1.4 \text{ pm}/\text{Hz}^{1/2}$  can currently only be achieved with an interferometer, realized with a resonance cavity. Because the nominal incidence angle of the PAAM is  $45^\circ$ , the cavity was made triangular. To keep the cavity resonant, the stabilized laser frequency that is generated in an external cavity is modulated by a controller. The actuator is an Electro-Optical Modulator, which is included in the vacuum chamber. The sensor is a frequency counter, which measures the resonance frequency of the cavity relative to the reference cavity. The feedback signal is a measure of the cavity round trip length change, which represents the contribution of the mechanism to the OPD. The cavity of the measurement set-up inside the vacuum chamber was mounted on a Zerodur base plate, to minimize the influence temperature variations on the cavity round trip length.

### Test description

Two of the critical requirements of the PAAM needed to be verified by tests: the OPD and the angular jitter. Both were measured at three different static angles within the range of the mechanism. The LISA measurement bandwidth determines the length of each performance measurement: the lowest frequency to be measured is 0.03 mHz. With several repetitions of this period to obtain a

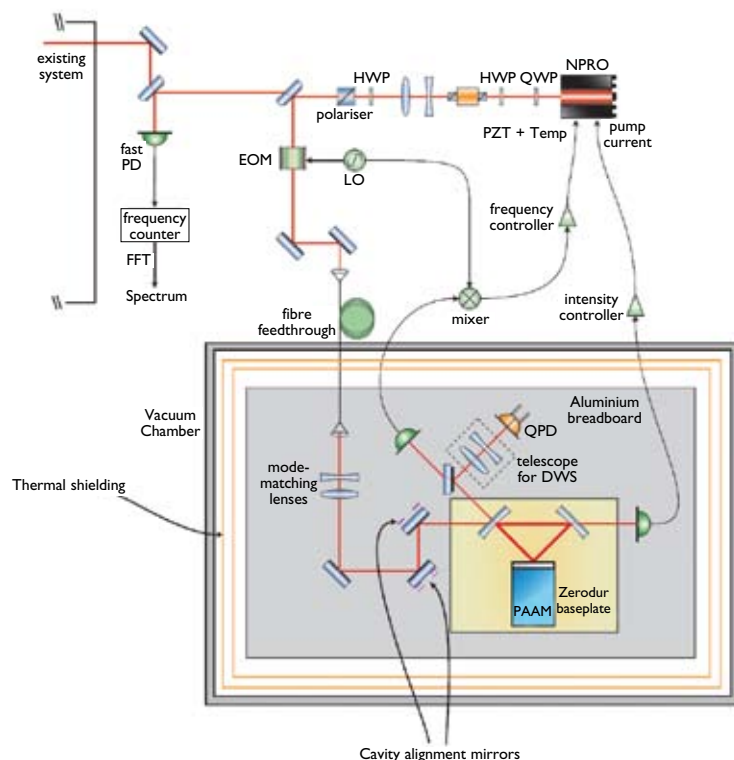


Figure 7. The OPD of the PAAM was measured in a triangular resonance cavity, inside a temperature-controlled vacuum tank. (Courtesy of Albert Einstein Institute, Hannover)

proper spectral estimate, the measurement time per angle was approximately 48 hours.

To measure the OPD, the PAAM had to be aligned accurately in the resonance cavity. To achieve this, a modulation sine wave was used as a setpoint on the mechanism, which followed this signal by rotation of the mirror. Through the amplitude of the sine wave, the misalignment of the axis of rotation with respect to the incoming beam could be estimated.

To measure the angular jitter, the PAAM was deliberately placed at an alignment offset. A modulation sine wave was used as a setpoint for the PAAM. Through the amplitude of the sine wave, the coupling of angular jitter to OPD could be estimated. A long measurement of OPD then provided an indirect measurement of the angular jitter of the PAAM.

### Test performance results

The results of the performance measurements of OPD and angular jitter are shown in Figures 8 and 9. For all angles, the performance of the mechanism was exactly according to the requirements. The peak visible at 50 mHz is the modulation sine wave which was used for alignment in the OPD measurements, and coupling estimation in the angular jitter measurements.

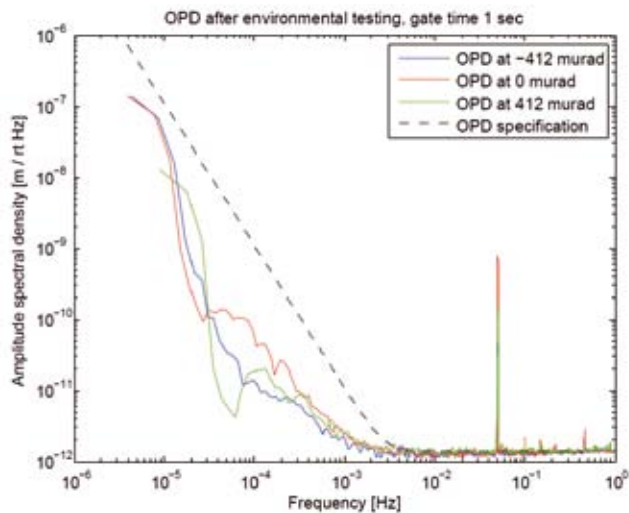


Figure 8. Amplitude Spectral Density of the OPD measurements on the PAAM. For all angles, the result met the requirements. The peak at 50 MHz was introduced for alignment in the cavity.

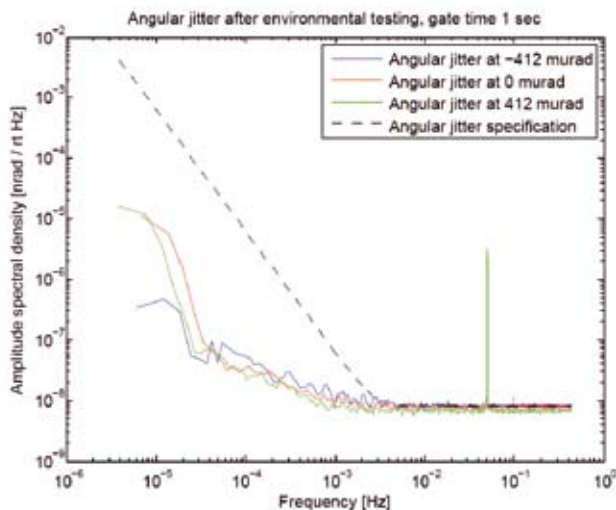


Figure 9. Amplitude Spectral Density of the angular jitter measurements on the PAAM. The PAAM was deliberately placed at an alignment offset, to make the angular jitter dominant in the OPD measurement. For all angles, the result met the requirements. The peak at 50 MHz was introduced to estimate the coupling of angular jitter to OPD.

## Evaluation

The PAAM concept has been based on a rotatable mirror. The critical requirements were the contribution to the optical path length (less than  $1.4 \text{ pm/Hz}^{1/2}$ ) and the angular jitter (less than  $8 \text{ nrad/Hz}^{1/2}$ ). Extreme dimensional stability was achieved by manufacturing a monolithic Haberland hinge mechanism out of  $\text{Ti}_6\text{Al}_4\text{V}$ , through high-precision wire erosion. Extreme thermal stability was realized by placing the thermal centre on the surface of the mirror. Because of piezo actuator noise and leakage, the PAAM has to be controlled in closed loop. To meet the requirements in the low frequencies, an active target capacitance-to-digital converter was used. Interferometric measurements with a triangular resonant cavity in vacuum proved that the PAAM meets the requirements.

## Conclusion

With the design, realization and testing of the PAAM, TNO Science and Industry has demonstrated that a scanning mechanism with picometer stability that has to operate under extreme environmental conditions is achievable. Performance test measurements have shown that it is compliant with the challenging requirements for optical path delay and angular jitter. The analysis, as well as the measurement results, showed that application of a Haberland hinge in a monolithical structure enables rotation with negligible parasitical motion in terms of optical path delay. The thermal design of the structure proved to be sufficient to guarantee the thermal stability. The angular jitter measurements have shown that an active target capacitive sensor system meets the extreme requirements on low-frequency noise. The Elegant Bread Board of the PAAM, as used in the performance testing, will be included in a breadboard model of the LISA Optical Bench in the near future.

## References

- [1] Danzmann, K., "LISA Mission Overview", *Advances in Space Research* Vol. 25, Issue 6, 2000, 1129-1136.
- [2] [lisa.nasa.gov](http://lisa.nasa.gov)
- [3] Troebs, M., "Laser development and stabilization for the spaceborne interferometric gravitational wave detector LISA", Ph.D. dissertation, 2005.